



# Synergistic effects of fiber debonding and fracture on matrix cracking in fiber-reinforced ceramic-matrix composites



Li Longbiao

College of Civil Aviation, Nanjing University of Aeronautics and Astronautics, No. 29 Yudao St., Nanjing 210016, PR China

## ARTICLE INFO

### Keywords:

Ceramic-matrix composites (CMCs)  
Matrix cracking  
Interface debonding  
Fiber failure

## ABSTRACT

In this paper, the synergistic effects of fiber debonding and fracture on matrix cracking stress of fiber-reinforced ceramic-matrix composites (CMCs) have been investigated using the energy balance approach. The shear-lag model cooperated with fiber/matrix interface debonding criterion and fiber fracture model has been adopted to analyze stress distribution in CMCs. The relationships between matrix cracking stress, interface debonding and slipping, and fiber fracture have been established. The effects of fiber volume fraction, interface shear stress, interface debonded energy, fiber Weibull modulus, and fiber strength on matrix cracking stress, interface debonded length and fiber broken fraction have been analyzed. The experimental matrix cracking stress of three different CMCs, i.e., SiC/borosilicate, SiC/LAS, and C/borosilicate, with different fiber volume fraction have been predicted.

## 1. Introduction

Ceramic materials possess high strength and modulus at elevated temperature. But their use as structural components is severely limited because of their brittleness. Continuous fiber-reinforced ceramic-matrix composites, by incorporating fibers in ceramic matrices, however, not only exploit their attractive high-temperature strength but also reduce the propensity for catastrophic failure. These materials have already been implemented on some aero engines' components [1]. The CMCs exhibit distinct behaviors at stresses above and below the matrix cracking stress, which is associated with the onset of matrix cracking and with the formation of hysteresis loops that results from matrix cracking and frictional slipping of the fibers bridging matrix cracks. In the environmentally-stable fibers and fiber coating in oxidizing environments, the matrix cracking stress has long been considered the maximum allowable design stress for CMCs in the real applications involving oxidizing environments.

Many researchers performed experimental and theoretical investigations on matrix cracking of fiber-reinforced CMCs. For analytical modeling, the energy balance approach developed by Aveston, Cooper and Kelly (ACK) [2], Budiansky, Hutchinson and Evans (BHE) [3], and Chiang [4], and the fracture mechanics approach proposed by Marshall, Cox and Evans (MCE) [5], and McCartney [6] have been used to investigate the matrix cracking stress. The analytical results show that the matrix cracking stress was closely related with the interface friction stress. The composite with the higher interface shear stress results in the higher matrix cracking stress. When the fiber/

matrix interface is weakly bonding, the BHE model will reduce to the ACK model, and when the interface is strongly bonding, the matrix cracking stress predicted by the BHE model is the same with that of Aveston and Kelly [7]. Rajan and Zok [8] investigate the mechanics of a fully bridged steady-state matrix cracking in unidirectional CMCs under shear loading. However, the models mentioned above do not consider the synergistic effects of fiber debonding and fracture on matrix cracking stress in CMCs.

During the process of matrix cracking in CMCs, the fiber/matrix interfacial debonding occurs due to the fiber-matrix relative displacement above the matrix cracking plane, and fibers failure also occurs due to the statistical properties of the fibers strength. In the present analysis, the shear-lag model is adopted to analyze the micro-stress field of the damaged composite, including the fiber, matrix and fiber/matrix interface shear stress in the interface debonded and bonded region. The Global Load Sharing criterion (GLS) and the fracture mechanics approach were used to determine the broken fibers fraction and the interface debonded length during matrix cracking. The effects of interface debonding and slipping, and fibers fracture have been taken into consideration to solve the matrix cracking stress. The influence of material properties, i.e., fiber volume fraction, interface shear stress, interface debonded energy, fiber Weibull modulus, and fiber strength on matrix cracking stress, interface debonded length and fiber broken fraction have been analyzed.

E-mail address: [llb451@nuaa.edu.cn](mailto:llb451@nuaa.edu.cn).

<http://dx.doi.org/10.1016/j.msea.2016.11.077>

Received 20 September 2016; Received in revised form 14 October 2016; Accepted 22 November 2016

Available online 23 November 2016

0921-5093/ © 2016 Published by Elsevier B.V.

## 2. Materials and experimental procedures

The three unidirectional fiber-reinforced CMCs for matrix cracking were provided by Barsoum et al. [9], including (a) the SiC/lithium/aluminosilicate (SiC/LAS) system, which comprises a SiC fiber (Nicalon, Nippon Carbon Co., Tokyo Japan) and a LAS matrix; (b) the carbon/borosilicate system, which is made of HMU carbon fibers (HMU Hercules carbon fiber) embedded in a borosilicate glass matrix; and (c) the SiC/borosilicate system, consisting of a SiC monofilament (SCS-6 SiC Fiber, Textron Specialty Materials, Lowell, Massachusetts, USA) embedded in the same borosilicate glass matrix. The variation in fiber volume fraction is achieved by controlling the amount of glass powder used in the preparation of the polymer slurry.

Three-point-bend test specimens were performed in the form of flat bars having the dimensions of  $3 \times 0.5 \times 0.18 \text{ cm}^3$  for SiC/LAS,  $3 \times 0.5 \times 0.2 \text{ cm}^3$  for C/borosilicate, and  $6 \times 0.5 \times 0.2 \text{ cm}^3$  for SiC/borosilicate. The pin-support span of the three-point bend fixture was 2.54 cm for the shorter bars and 5.2 cm for the longer bars. During the three-point-bend testing, the maximum beam deflection was measured with an extensometer mounted at the beam mid-span; at the same time, the electrical resistance of the gold film sputtered on the polished specimen surface was measured with a digital Ohm meter. The deflection and electrical resistance were recorded as a continuous function of loading and were then used to determine the onset of the matrix cracking stress.

## 3. Stress analysis

When fibers break during matrix cracking, the loads dropped by the broken fibers must be transferred to the intact fibers in the cross-section. Two dominant failure criteria are present in the literatures for modeling fibers failure, i.e., Global Load Sharing criterion (GLS) and Local Load Sharing criteria (LLS). The GLS criterion assumes that the load from any one fiber is transferred equally to all other intact fibers in the same cross-section plane. The GLS assumption neglects any local stress concentrations in the neighborhood of existing breaks, and is expected to be accurate when the interfacial shear stress is sufficiently low. Models that include GLS explicitly have been developed, which includes Thouless and Evans [10], Cao and Thouless [11], Sutcu [12], Schwietert and Steif [13], Curtin [14], Weitsman and Zhu [15], Hild et al. [16], Solti et al. [17], Cho [18], Paar et al. [19], Liao and Reifsnider [20], and so on. The LLS assumes that the load from the broken fiber is transferred to the neighborhood intact fibers, and is expected to be accurate when the interface shear stress is sufficiently high. Models that include LLS explicitly have been developed, which includes Zhou and Curtin [21], Dutton et al. [22], Xia and Curtin [23], and so on.

The two-parameter Weibull model is adopted to describe the fiber strength distribution, and the Global Load Sharing (GLS) assumption is used to determine the load carried by intact and fracture fibers [14].

$$\frac{\sigma}{V_f} = T [1 - P(T)] + \langle T_b \rangle P(T) \tag{1}$$

where  $V_f$  denotes the fiber volume fraction;  $T$  denotes the load carried by intact fibers;  $\langle T_b \rangle$  denotes the load carried by broken fibers; and  $P(T)$  denotes the fiber failure probability.

$$P(T) = 1 - \exp \left[ - \left( \frac{T}{\sigma_c} \right)^{m+1} \right] \tag{2}$$

where  $m$  denotes the fiber Weibull modulus; and  $\sigma_c$  denotes the fiber characteristic strength.

The load carried by broken fibers is determined by the Eq. (3).

$$\langle T_b \rangle = T \left[ \left( \frac{\sigma_c}{T} \right)^{m+1} - \frac{1 - P(T)}{P(T)} \right] \tag{3}$$

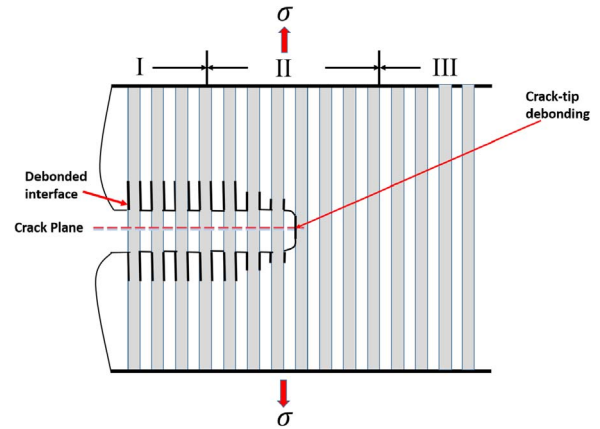


Fig. 1. The schematic of crack-tip and interface debonding.

Substituting Eqs. (2) and (3) into the Eq. (1), it leads into the form of

$$\frac{\sigma}{V_f} = T \left( \frac{\sigma_c}{T} \right)^{m+1} \left\{ 1 - \exp \left[ - \left( \frac{T}{\sigma_c} \right)^{m+1} \right] \right\} \tag{4}$$

Using the Eq. (4), the stress  $T$  carried by intact fibers at the matrix cracking plane can be determined. Substituting the intact fiber stress  $T$  into the Eq. (2), the relationship between the fiber failure probability and applied stress can be determined.

### 3.1. Downstream stresses

The composite with fiber volume fraction  $V_f$  is loaded by a remote uniform stress  $\sigma$  normal to a long crack plane, as shown in Fig. 1. The unit cell in the downstream Region I contained a single fiber surrounded by a hollow cylinder of matrix is extracted from the ceramic composite system, as shown in Fig. 2. The fiber radius is  $r_f$ , and the matrix radius is  $R$  ( $R = r_f / V_f^{1/2}$ ). The length of the unit cell is half matrix crack spacing  $l_c/2$ , and the interface debonded length is  $l_d$ . In the debonded region, the interface is resisted by  $\tau_i$ . For the debonded region in Region I, the force equilibrium equation of the fiber is given by Eq. (5) [3].

$$\frac{d\sigma_f(z)}{dz} = - \frac{2\tau_i(z)}{r_f} \tag{5}$$

The boundary conditions of the fiber and matrix axial stresses at the crack plane (i.e.,  $z=0$ ) are given by

$$\sigma_f(z=0) = T \tag{6}$$

$$\sigma_m(z=0) = 0 \tag{7}$$

The total axial stresses in Region I satisfy the Eq. (8).

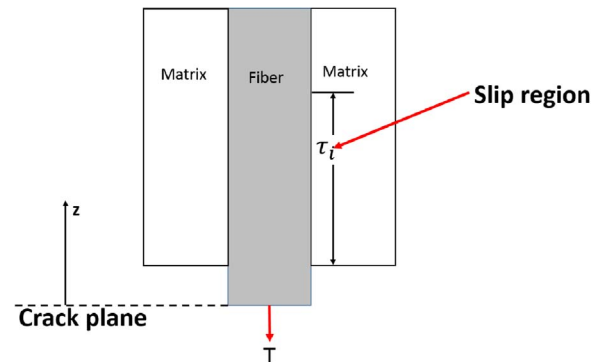


Fig. 2. The schematic of shear-lag model considering interface debonding.

Download English Version:

<https://daneshyari.com/en/article/5456423>

Download Persian Version:

<https://daneshyari.com/article/5456423>

[Daneshyari.com](https://daneshyari.com)